Resonances and virtual states for a quantum tunnelling model

1989 J. Phys. A: Math. Gen. 22 2667

(http://iopscience.iop.org/0305-4470/22/14/017)

J. Phys. A: Math. Gen. **22** (1989) 2667-2674. Printed in the UK

Resonances and virtual states for a quantum tunnelling model

P J Hofstee†, H G Muller and A Tip

FOM-Institute for Atomic and Molecular Physics, Kruislaan 407, 1098 SJ Amsterdam, The Netherlands

Received 5 August 1988, in final form 23 February 1988

Abstract. For a quantum particle moving in the combined field of a negative δ potential and a negative step potential, respectively a semi-infinite Kronig-Penney lattice, the behaviour of a resonance pole is studied as a function of the distance between the centre of the δ potential and the step, respectively lattice. It is found that as this distance is decreased the resonance changes into a virtual state in both cases. In the Kronig-Penney case, however, the situation can become more complicated, particularly if there exists a band gap below zero.

1. Introduction

The stability of eigenvalues of a quantum system under a parameter change in the Hamiltonian is a subject with a long history. One of the best known cases is that of a three-dimensional Schrödinger particle moving in a sufficiently regular attractive central potential γV, $\gamma > 0$. Here, if γ is decreased, eigenvalues supported by V eventually disappear, but the situation is different for s states ($l = 0$) and higher angular momentum states ($l = 1, 2, \ldots$). In the $l = 0$ case an eigenvalue first turns into a virtual state before becoming a resonance, whereas for $l > 0$ a direct change into a resonance takes place (see, for instance, Newton 1966). In general, however, such specific information is usually not available. In the present paper we discuss two simple one-dimensional systems which exhibit a transition from a virtual state into a resonance, akin to the s-state case above. The first model, studied in § 2, is that of a particle moving in a combination of an attractive δ potential and a step potential ($\Theta(x) = 1$ for $x \geqslant 0$ and $\Theta(x) = 0$ otherwise):

$$V(x) = -\lambda\delta(x - y) - \mu\Theta(x) \qquad \lambda, \mu > 0 \tag{1.1}$$

where $-y > 0$, the distance between the centre of the δ potential and the step is the parameter which will be varied. Without the step ($\mu = 0$) $V(x)$ supports a bound state with eigenvalue $E = -\frac{1}{4}\lambda^2$. In case $\frac{1}{4}\lambda^2 \leqslant \mu$, $V(x)$ no longer supports a bound state. Here we encounter a typical quantum tunnelling situation where a particle originally centred on the δ potential can tunnel to the right into the region where the step potential is effective. As discussed in detail in § 2, we now have the following situation. For y sufficiently large negative there exists a single resonance $E(y)$ which tends to E as $y \to -\infty$. For increasing but still negative y, $E(y)$ turns into a pair of virtual states, one of which eventually becomes a bound state with asymptotic value $E - \mu$ as $y \to \infty$

† Present address: Centre for Mathematics and Information Science, Kruislaan 413, 1098 SJ Amsterdam, The Netherlands.

0305-4470/89/142667+08$02.50

(the other tends to $-\infty$). Thus the situation is similar to the $l=0$ case above (but note that we do not simply change the strength of a potential). In order to see whether the situation is specific to the potentials chosen, we replaced the step potential by a semi-infinite Kronig-Penney lattice. As discussed in § 3, again a transition from a resonance into a pair of virtual states is found. In this case, however, a second resonance appears, which shows a quite spectacular behaviour if there is a band gap below zero. We close our paper with § 4, where a short discussion of our results, and possible generalisations, is given. Related papers, concerning similar tunnelling situations, are Caroli *et al* (1972), Hurault (1971) and Knauer *et al* (1977). These treatments are not restricted to the one-dimensional situation. On the other hand, the case of a lattice is not considered nor is the transition to a virtual state studied in detail. The general properties of infinitely many δ interactions in one dimension are thoroughly discussed by Albeverio *et al* (1988). Other recent results, specifically for eigenvalues of δ potential models can be found in Ushveridze (1988). The mathematical literature on stability of eigenvalues and resonances has conveniently been summarised in Reed and Simon (1978, notes to chapter XII); see also Simon (1977).

2. The step potential case

In this section we study the resonance that originates from the eigenvalue $-\lambda^2/4$ of $H_1=-\partial_x^2-\lambda\delta(x-y)$ under the perturbation $-\mu\Theta(x)$. The full Hamiltonian is

$$H=-\partial_x^2-\mu\Theta(x)-\lambda\delta(x-y)=H_0-\lambda|y\rangle\langle y| \qquad \lambda,\mu>0 \tag{2.1}$$

with

$$H_0=-\partial_x^2-\mu\Theta(x). \tag{2.2}$$

Its resolvent is

$$[z-H]^{-1}=[z-H_0]^{-1}-\Gamma(z,y)^{-1}[z-H_0]^{-1}|y\rangle\langle y|[z-H_0]^{-1} \tag{2.3}$$

where

$$\Gamma(z,y)=\lambda^{-1}+\langle y|[z-H_0]^{-1}|y\rangle. \tag{2.4}$$

Eigenvalues and resonances are associated with the zeros of $\Gamma(z,y)$ as a function of z (the latter after continuation in a higher Riemann sheet). The Green function $G(x,x',z)=\langle x|[z-H_0]^{-1}|x'\rangle$ is easily calculated, with the result

$$\Gamma(z,y)=\begin{cases}\lambda^{-1}-(2\mathrm{i}\kappa)^{-1}\left(1+\dfrac{\kappa-\kappa_\mu}{\kappa+\kappa_\mu}\exp(-2\mathrm{i}\kappa y)\right) & y\leqslant 0\\ \lambda^{-1}-(2\mathrm{i}\kappa_\mu)^{-1}\left(1-\dfrac{\kappa-\kappa_\mu}{\kappa+\kappa_\mu}\exp(2\mathrm{i}\kappa_\mu y)\right) & y\geqslant 0.\end{cases} \tag{2.5}$$

Here $\kappa=\sqrt{z}$ and $\kappa_\mu=\sqrt{z+\mu}$ and in the case $\mu=0$ we recover the zero $E=-\lambda^2/4$. The points $z=0$, $-\mu$ and ∞ are branch points of Γ and we encounter four different Riemann sheets. Relevant to us is the sheet in which an, in general, complex zero $E(y)$ with non-positive imaginary part can be found, which tends to $-\frac{1}{4}\lambda^2$ as y becomes large negative. An elegant precise prescription is possible, using complex dilatation arguments (Hofstee and Tip 1988). After complex dilatation the continuous spectrum of H changes into two branches, the semi-axis $[0,\infty)$ and a second branch consisting of a ray in the lower half-plane starting at $-\mu$. Now, analytic continuation of the

resolvent through the gap $(-\mu, 0)$ is possible and it is the pole of this continuation that we are interested in. Since the dilated resolvent has a structure similar to (2.3) *with the same* $\Gamma(z, y)$, this procedure tells us which Riemann sheet must be considered.

We now turn to the numerical results. Obviously the interesting parameter range is the one with $0 < \lambda^2/4 \leq \mu$ since for $\lambda^2/4 > \mu$ the bound state remains. We considered the case $\lambda = 2$, so that $\lambda^2/4 = 1$ and a range of μ values between 1.5 and 8. For

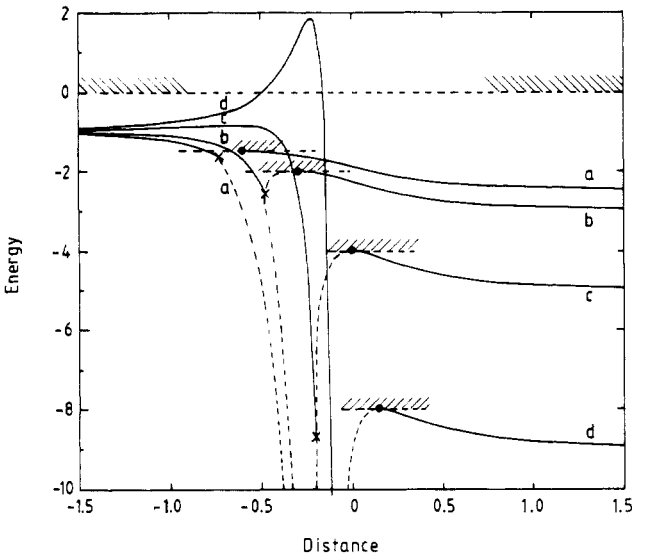

Figure 1. Delta function of strength $\lambda = 2$ before a step potential of various magnitudes μ; a: $\mu = 1.5$, b: $\mu = 2$, c: $\mu = 4$ and d: $\mu = 8$. The real part of the resonance energy is plotted as a function of the distance between the step and the delta centre; positive distance means that it is inside the step potential. On the left the full curves represent a resonance, on the right a bound state. The broken curves represent virtual states. The position of the continua are indicated by hatching: // is the continuum starting at $-\mu$, \\ the continuum starting at zero.

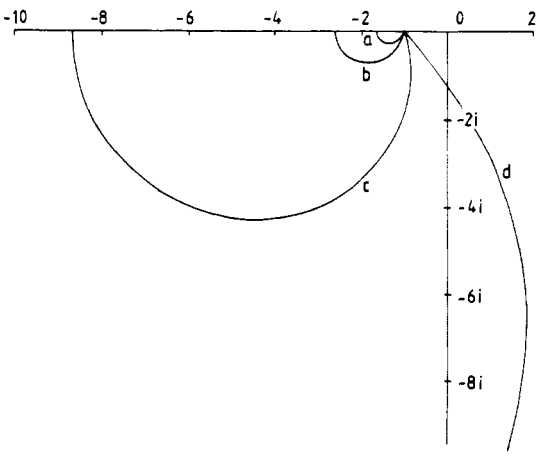

Figure 2. Delta function before a step potential of various magnitudes μ. The trajectory of the resonances in the complex plane is shown for a: $\mu = 1.5$, b: $\mu = 2$, c: $\mu = 4$ and d: $\mu = 8$.

sufficiently negative y we indeed find a complex zero $E(y)$ of $\Gamma(z, y)$ in the lower half-plane. In figure 1 its real part is plotted as a function of y. Negative y corresponds to a δ potential centred outside the step potential and for positive y its centre is inside the step potential. Starting at large negative y, Re $E(y)$ is close to -1 and starts to decrease for small μ but increases and even becomes positive for large μ. In figure 2 the corresponding orbit of $E(y)$ in the complex plane is given. We note that eventually $E(y)$ returns to the real axis. Once this happens it breaks up into a set of two virtual states, i.e. real zeros of Γ but not in the physical Riemann sheet (so that no square-integrable eigenfunctions can be associated with them). Decreasing $|y|$ still further, one virtual state moves away to $-\infty$ as $y \uparrow 0$ and the other one moves upwards to the bottom of the continuous spectrum $-\mu$ of H (the broken curves in figure 1). After hitting $-\mu$ the second zero remains real but now becomes a proper eigenvalue $< -\mu$ of H and it remains an eigenvalue for all larger y with the asymptotic value $-\mu - \lambda^2/4$. This reflects the intuitive idea that far to the right (large positive x) the influence of the step at $x = 0$ becomes negligible.

3. The Kronig–Penney case

In order to see whether the appearance of a virtual state is specific for a step potential we replaced the latter by a Kronig-Penney (KP) lattice on a half-axis. The only difference with the formulae of § 2 is the corresponding change of H_0, which now is the Hamiltonian for a semi-infinite KP lattice

$$H_0 = -\partial_x^2 - \nu \sum_{n=1}^{x} \delta(x - nR) \qquad \nu > 0 \tag{3.1}$$

where $R > 0$ is the lattice distance and the first lattice position is $x = R$, which is a better choice than $x = 0$ for comparisons with the step potential case as discussed in the following. Also, for comparison reasons, we shall choose ν and R in such a way that the bottom of the lowest (negative) band coincides with $-\mu$ of § 2. Again we can calculate the Green function associated with (3.1) and subsequently determine the relevant zeros of $\Gamma(z, y)$. (In this case, however, no complex dilatation theory exists, which enables us to associate the zeros of Γ with eigenvalues of the dilated Hamiltonian.) In the appendix its precise form is given. It is known (Albeverio *et al* 1988, chapter III.2.4, theorem 2.4.1) that the semi-infinite KP lattice has a purely absolutely continuous spectrum consisting of the union of the free particle spectrum $[0, \infty)$ and the band spectrum of the full KP lattice. In particular, surface bound states are absent.

The Green function associated with (3.1) has a more complicated structure than the one corresponding to (2.1). Like the infinite KP lattice the semi-infinite array has a band structure in its spectrum, the band edges corresponding to branch points of the Green function. For $\nu > 0$ the bottom of the lowest band is at $-\mu < 0$, with μ depending on ν, and if $\nu R = 4$ the top of this 'valence' band lies at 0. In the latter case it coincides with the branch point in the Green function at zero, which is due to the presence of a semi-infinite vacuum region in front of the lattice (leading to a branch $[0, \infty)$ of the spectra of H_0 and H). For larger values of νR there exists a band gap between the bottom of the valence band and 0.

Even though the Green function has an infinite number of branch points, there are only four different Riemann sheets associated with its analytic continuations. They

can be labelled in terms of the four possible combinations of boundary conditions (decaying or blowing up) in $x = \pm\infty$.

First we consider the case without a band gap ($\nu R = 4$), again for different values of μ, ranging from 1 to 2. Starting from $y = -\infty$, $E(y)$ changes from its asymptotic value $-\lambda^2/4$ into a point in a higher Riemann sheet for finite large negative y and thus corresponds to a resonance. Its real part is plotted in figure 3 and its orbit in the complex plane in figure 4. For $\mu < 1.38$ its behaviour is similar to the step-potential case (curve b in the figures). If the lattice potentials are identical to the one in front, i.e. $\lambda = \nu$, we have a critical case, $\mu = 1.38$, where the situation with $y = 0$ is indistinguishable from a semi-infinite lattice (with $y = 0$ the first lattice position). Now all resonances and virtual states move to infinity as $y \uparrow 0$.

For still larger values of μ (supercritical case) the resonance behaviour changes drastically. Instead of bending to the real axis and changing into a virtual state below $-\mu$, $E(y)$ now heads for the (double) branch point 0 as y increases. It then 'dives' through this point and changes into a resonance in a third Riemann sheet, corresponding to a state that decays by emission of a particle into the vacuum instead of being transferred to the lattice. Also in this case a bound state appears below $-\mu$. It comes into existence when a virtual state moving up from $z = -\infty$ (where it appears for $y = 0$), hits $-\mu$ and switches to the physical Riemann sheet. (Note that the particle only hits the first lattice position for $y = R$.)

If a band gap is present, the behaviour of the resonance in the supercritical case becomes quite spectacular. In figure 5 the orbit $E(y)$ and its real part are plotted. As y increases to zero, $E(y)$ now hits the real axis in the band gap and splits into two virtual states. Both eventually hit a branch point. One crosses over at the top of the

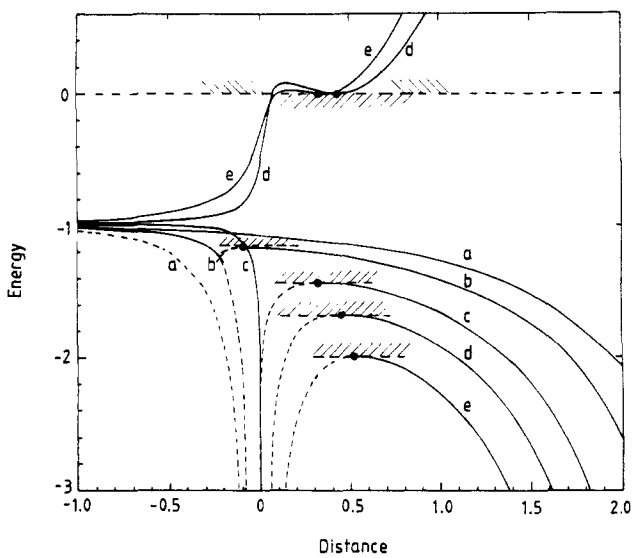

Figure 3. Delta function before a Kronig-Penney lattice of various magnitude μ; a: $\mu = 1$, b: $\mu = 1.11$, c: $\mu = 1.38$ (the critical case), d: $\mu = 1.70$ and e: $\mu = 2.00$. The real part of the resonance energy is plotted as a function of the distance between the first unoccupied lattice position and the delta centre; positive distance means that the centre is closer to the crystal than one lattice constant. On the left the full curves represent a resonance, on the right a bound state. The broken curves represent virtual states. Hatching \\ indicates the vacuum band, and // the valence band.

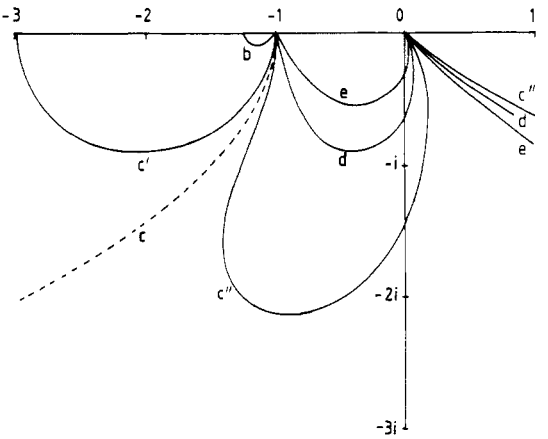

Figure 4. Delta function before a Kronig-Penney lattice of various magnitudes μ. The trajectory of the resonances through the complex plane is shown for the cases a to e of figure 3, as well as two cases near the critical one, c' and c''. The curve for the critical case extends to infinity, and separates the plane into two regions. Curves in the left region behave qualitatively the same as the step case (figure 2), but curves belonging to supercritical cases (living in the right region) turn back to the origin, where they change into resonances of a different nature.

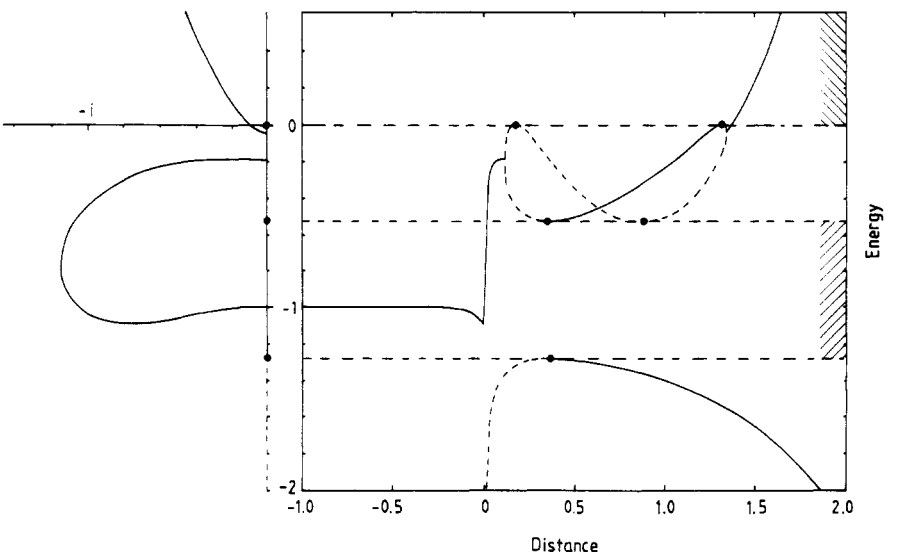

Figure 5. A similar case to curve d of figure 3, but now for a Kronig-Penney lattice with a band gap. On the right side the real part of the energy is plotted as a function of distance, on the left side the corresponding imaginary part can be found whenever the state is a resonance. The full curves represent either resonances (left and upper right), or bound states (middle and lower right). The broken curves represent virtual states. For a detailed discussion of the behaviour in the band gap we refer to the text. The meaning of the hatching is the same as in figure 3.

valence band into the physical Riemann sheet and turns into a true bound state. (Since there is a second bound state with energy below $-\mu$ we now have bound states at both sides of the valence band.) The other virtual state moves through zero into the fourth Riemann sheet (specified by the 'blowing up' boundary condition in both $\pm\infty$). This virtual state, as well as the bound state, traverses the entire band gap, collides with the band edges and changes into virtual states, which then coalesce into a resonance that decays by particle emission. In summary we note that for large negative y the situation is similar to the step-potential case but closer in, depending on the choice of parameters, a more complicated behaviour can occur.

4. Discussion

In §§ 2 and 3 we found that for sufficiently large negative distances a bound state turns into a resonance due to the presence of a step potential or a semi-infinite Kronig–Penney lattice. Closer in, we saw the transition of the resonance into a virtual state, resembling the situation in s-wave potential scattering. The question arises whether this situation is specific for our models. In our opinion a change from a δ interaction into some more general potential $V(x)$ and a change into a lattice different from the KP one should not affect these results. This conjecture could eventually be tested by developing a formalism of the Jost function type for the case at hand. In three dimensions, however, the situation may change. Much will depend on existing symmetries in the half-lattice and it may well be that various types of behaviour can be distinguished. This case is not without physical interest since the transfer of electrons between atoms and metal surfaces (see, for instance, van Wunnik *et al* 1983) is governed by a similar tunnelling process.

Acknowledgments

Useful discussions with J J C Geerlings and J Los are gratefully acknowledged. This work is part of the research program of the Stichting voor Fundamenteel Onderzoek der Materie (Foundation for Fundamental Research of Matter) and was made possible by financial support from the Nederlandse Organisatie voor Wetenschappelijk Onderzoek (Netherlands Organisation for the Advancement of Research).

Appendix. The Green function for the semi-infinite Kronig–Penney lattice

Here we give an expression for the Green function (integral kernel associated with the resolvent) for the semi-infinite Kronig–Penney lattice. Let

$$H_1 = -\partial_x^2 - \gamma \sum_{n=0}^{\infty} \delta(x-n) \qquad \gamma \text{ real} \tag{A1}$$

which is H_0 of equation (3.1) modulo a scaling and a shift. The associated Green function is

$$G(x, x', \kappa) = \langle x|[z - H_1]^{-1}|x'\rangle \qquad \kappa = \sqrt{z} \qquad \operatorname{Im}\kappa > 0. \tag{A2}$$

We note that $G(x, x', \kappa) = \overline{G(x', x, -\bar{\kappa})}$ and that G can be obtained in the usual way from the Schrödinger equation with an inhomogeneous term of the δ function type added. Outside the points $1, 2, 3, \ldots$ we have the free-particle solution and within these points the familiar jump condition on the derivative of G with respect to x and x'. This, together with continuity requirements and boundedness for large argument, fixes G completely. The result is

$$G(x, x', \kappa) = \begin{cases} [2i\kappa)^{-1}\{\exp[i\kappa|x-x'|] + b_- \exp[-i\kappa(x+x')]\} & x, x' \in I_0 \\ [2i\kappa]^{-1}\rho_-^n\{\exp[i\kappa(x-n)] + b_- \exp[-i\kappa(x-n)]\} & \\ \qquad \times \exp[-i\kappa x'] \qquad x \in I_n,\ x' \in I_0 & \\ [2i\kappa]^{-1}\rho_-^n\{\exp[i\kappa(x-n)] + b_- \exp[-i\kappa(x-n)]\}\{r_m \exp[i\kappa(x'-m)] & \\ \qquad + s_m[-i\kappa(x'-m)]\} \qquad x \in I_n, x' \in I_m \qquad n > m \end{cases} \tag{A3}$$

where $I_0 = (-\infty, 0)$, $I_n = (n-1, n)$, $n = 1, 2, 3, \ldots$ and

$$b_\pm = \exp[\pm i\kappa]a \qquad a = \frac{i\gamma}{2\kappa}\left[\left(1 - \frac{i\gamma}{2\kappa}\right)\exp[-i\kappa] - \rho_-\right]$$

$$r_m = b_+(a^2-1)(\rho_-^m - \rho_+^m) \qquad s_m = (a^2-1)(a^2\rho_-^m - \rho_+^m) \tag{A4}$$

$$\rho_\pm = \sigma \pm \sqrt{\sigma^2 - 1} \qquad \sigma = \frac{1}{2}\left[\left(1 + \frac{i\gamma}{2\kappa}\right)\exp[i\kappa] + \left(1 - \frac{i\gamma}{2\kappa}\right)\exp[-i\kappa]\right].$$

Note that in the main text we only require $G(x, x, \kappa)$ for negative x.

References

Albeverio S, Gesztesy F, Høegh-Krohn R and Holden H 1988 *Solvable Models in Quantum Mechanics* (Berlin: Springer)

Caroli C, Lederer D and Saint James D 1972 *Surf. Sci.* **33** 228

Hofstee P J and Tip A 1988 *J. Math. Phys.* **29** 817

Hurault J P 1971 *J. Physique* **32** 421

Knauer H, Richter J and Seidel P 1977 *Phys. Status Solidi* **44** 303

Newton R G 1966 *Scattering Theory of Waves and Particles* (New York: McGraw-Hill)

Reed M and Simon B 1978 *Methods of Mathematical Physics IV, Analysis of Operators* (New York: Academic)

Simon B 1977 *J. Funct. Anal.* **25** 338

Ushveridze A G 1988 *J. Phys. A: Math. Gen.* **21** 955

van Wunnik J N M and Los J 1983 *Phys. Scr.* **T6** 27